The 7th World Congress on Particle Technology (WCPT7)

SPH-Based Simulations for Slope Failure Considering Soil-Rock Interaction

Qiang Wu, Yi An, and Qing-quan Liu[*]

Key Laboratory for Mechanics in Fluid Solid Coupling Systems,
Institute of mechanics, Chinese Academy of Sciences, Beijing, 100190, China

Abstract

Both small and large deformations of soil and soil-rock interaction are the key features in the post-failure process of natural slopes. As one of Lagrange meshless particle methods, the Smooth Particle Hydrodynamics (SPH) method has obvious advantage in dealing with the large deformation and interface interaction problems. Thus in this paper, the SPH method is employed to study the slope failure problems, especially focusing on soil large deformation and soil-rock interaction in natural slopes constituted of earth-rock aggregate. The Drucker-Prager model is implemented into the SPH-code to describe the elastic-plastic soil behavior while the rocksare simulated as rigid bodiesby using classical rigid motion equations. The interaction between soil and rocksis modeled by the coupling condition associated with an action and reaction force between the two phases. Rock-rock contacts are computed using contact mechanics theory which issimilar to the treatment in the Discrete Element Method (DEM).Two test cases including uniform non-cohesive and cohesive soil slopes failure problems are studied respectively to validate the method and a good agreement with the experimental data or numerical results is observed. Then the solutionto soil-rock interaction is applied to study the behavior of earth-rock aggregate in the failure process of typical natural landslides. Numerical results show that the proposed soil-rock interaction algorithm works well in the SPH framework and has a great application potential in geotechnical engineering. Through the qualitative analysis and discussions about the behavior of earth-rock aggregate,we came to the conclusion thatthe soil-rock interaction has a great influence on the landslide shapein terms of rock size and slope angle.And the deformation characteristics of landslide at the slope toe isslightlydifferent with that at the slope top.

Keywords: SPH method; slope failure; earth-rock aggregate; large deformation; soil-rock interaction

*Corresponding author (E-mail address:*qqliu@imech.ac.cn).

1. Introduction

The slope failure usually has the destructive potential both in terms of human lives and their property,as demonstrated by the landslide that hit AfghanistanMay 2014. Therefore, the research on time prediction of slope failure is significant. As weknown, natural slopes generally consist of earth-rock aggregate. In the event oflandslide, the earth-rock aggregate easily produces fluidity and the soil inevitably interacts with the rocks.Thus it can be seen both small and large deformations of soil and soil-rock interaction are the key features in the post-failure process of natural slopes.

The earth-rock aggregate is a kind of special geological material between soil mass and rock mass, which has the non-linear property withobvious discontinuity, irregularity, and uncertainty. So it is difficult to utilize the traditional numerical method to make practical description and analyzeits peculiar geological and mechanical behavior.For example, the finite element Method (FEM)may suffer from the grid distortion problem, which need labored work to overcome.The discrete element method (DEM) could be better in dealing with these large deformation and significant flow problems.But for the continuous granular material, DEM would notoutperform FEM in calculation accuracy. In addition, the specification of DEM parameters is somewhat ambiguous, andreliable guidelines haven't yet to be clearly established[1].

The Smooth Particle Hydrodynamics (SPH) method has several advantages in dealing with large deformation of continuum or dispersed material and the interface interaction problems. The SPH method is a purely Lagrange meshless method in which particlescarry field variables such as mass, density, stress tensor, etc. and move with the material velocity[2]. It can handle largedeformation and post-failure very well due to its Lagrangian and adaptive nature; complex freesurfaces are captured naturally without any special treatments; complex geometries and interface interaction can be treatedrelatively easily.Fortunately, Bui et al.[1] has implemented elastic-plastic soil constitutive models in SPH code which availably solved plastic soil behavior. Afterwards, Opez, Y.R.L. et al.[3] proposed a dynamic refinementprocedure to reduce the computational requirements of an elastic-plastic model to simulate non-cohesive soil. They demonstrated that SPH has good performance to simulate large deformation and post-failure problems such as slope failures, landslides, particle flows that are common in geotechnical engineering.

The motivation of this paper is to discuss that how the earth-rock aggregate affects the deformation characteristics of slope failure. The post-failure with soil-rock and rock-rock interaction involves both small and large deformations.Considering the advantages of SPH method, this paper exploited it to simulate slope failure process and the soil-rock interaction.To begin with, based on elastic-plastic soil model, we establish a soil-rock interaction procedure in the DualSphysicscode[4~6](www.dual.sphysics.org), which allows to study more details about the behavior of the earth-rock aggregate.Then, two test cases including uniform non-cohesive and cohesive soil slope failures subjected to gravitational loading are simulated respectively to validate the method and good agreements with the experimental data or numerical results are observed. Finally, this method is employed to study the mechanics in failure process of typical natural slope constituted of earth-rock aggregate.

Nomenclature

α, β	Greek superscriptsdenoting Einstein's notation
i, j	Latin subscripts denotingindividual particles
$f_g, \delta^{\alpha\beta}$	gravitational acceleration and the Dirac delta function, respectively
m, ρ, v, x	mass, density, velocity and position of a soil particle, respectively
$M, V, \Omega,$	mass,velocity and rotational velocity of a rock, respectively
I, R_0	the moment of inertia and the position of the centre of rock mass,respectively
σ, ε	the total stress and strain tensor, respectively
c, φ	the Coulomb's material constants: cohesion and internal friction angle
f, g	the yield and plastic potential function, respectively
E, υ	Young's modulus and Poisson's ratio, respectively
G, K	the shear modulus and the elastic bulk modulus, respectively
I_1, J_2	the first and second invariants of the stress tensor, respectively
$W, h, \Delta d$	the cubic spline kernel function, the smoothing length and the initial particle spacing, respectively

| f_{rs} | the force per unit mass exerted by soil particle s on rock particle r |
| SPs, RPs | soil particles and rock particles within smoothed kernel, respectively |

2. SPH formulation

In this section, we first formulate the basicgoverning equationsfor soil. Then, we briefly describe an elastic-plastic soil model based on the Drucker-Prageryield condition in the SPH framework. More details can be found in the originalworkby Bui et al[1].Finally, we present the SPH implementation of soil-rock interaction.

2.1. Continuity and momentum equations

The continuity equation in SPH can be expressed as

$$\frac{D\rho_i}{Dt} = \sum_{j=1}^{N} m_j (v_i^{\alpha} - v_j^{\alpha}) \frac{\partial W_{ij}}{\partial x_i^{\alpha}} \tag{1}$$

Themomentum equation can be described by the following SPH discretization:

$$\frac{Dv_i^{\alpha}}{Dt} = \sum_{j=1}^{N} m_j (\frac{\sigma_i^{\alpha\beta} + \sigma_j^{\alpha\beta}}{\rho_i \rho_j} - \Pi_{ij} \delta^{\alpha\beta} + F_{ij}^{\ n} R_{ij}^{\ \alpha\beta}) \frac{\partial W_{ij}}{\partial x_i^{\beta}} + f_g^{\alpha} \tag{2}$$

The artificial viscosity term Π is used to stabilize the numerical system. It is given by

$$\Pi_{ij} = \begin{cases} \dfrac{-\alpha c \mu_{ij} + \beta \mu_{ij}^2}{\bar{\rho}_{ij}} & v_{ij} \cdot x_{ij} < 0 \\ 0 & v_{ij} \cdot x_{ij} \geq 0 \end{cases}, \tag{3}$$

where $\mu_{ij} = \dfrac{h v_{ij} \cdot x_{ij}}{x_{ij}^2 + 0.01 h^2}$, $\bar{\rho}_{ij} = \dfrac{\rho_i + \rho_j}{2}$,α and β areconstants respectively taken to be 0.1 and 0 here.

The artificial stress methodrefer to the term $F_{ij}^{\ n} R_{ij}^{\ \alpha\beta}$ is applied to reduce tensileinstabilities.The treatment is completely the same as suggested in the article[1].

2.2. The Drucker-Pragersoil model

For elastic-plastic materials, the strain rate tensor isnormallycomposed of two parts, the elastic $\dot{\varepsilon}_e^{\alpha\beta}$ and the plastic $\dot{\varepsilon}_p^{\alpha\beta}$ strain rate tensors, resulting in

$$\dot{\varepsilon}^{\alpha\beta} = \dot{\varepsilon}_e^{\alpha\beta} + \dot{\varepsilon}_p^{\alpha\beta} \tag{4}$$

The elastic term can be calculated by the generalized Hooke's law:

$$\dot{\varepsilon}_e^{\alpha\beta} = \frac{\dot{s}^{\alpha\beta}}{2G} + \frac{1-\upsilon}{3E} \dot{\sigma}^{\gamma\gamma} \delta^{\alpha\beta} \tag{5}$$

The plastic part can be computed by using the plastic flow rule:

$$\dot{\varepsilon}_p^{\alpha\beta} = \dot{\lambda} \frac{\partial g}{\partial \sigma^{\alpha\beta}} \tag{6}$$

The Drucker-Prageryield condition is applied here to determine the soil plastic flow regime. Accordingly, the plastic deformation will occur only if the following yield criterion is satisfied

$$f(I_1, J_2) = \sqrt{J_2} + \alpha_\varphi I_1 - k_c = 0 \tag{7}$$

α_φ and k_c are the Drucker-Prager's constants, in plane strain condition, are computed by

$$\alpha_\varphi = \frac{\tan\varphi}{\sqrt{9 + 12\tan^2\varphi}} \text{ and } k_c = \frac{3c}{\sqrt{9 + 12\tan^2\varphi}} \tag{8}$$

The non-associated plastic flow rule specifies the plastic potential function by

$$g(I_1, J_2) = \sqrt{J_2} + \alpha_\psi I_1 - \text{constant} \tag{9}$$

α_φ is similar to α_φ, given by

$$\alpha_\psi = \frac{\tan\psi}{\sqrt{9 + 12\tan^2\psi}} \tag{10}$$

The rate of change of the plastic multiplier λ is obtained by solving

$$\dot{\lambda}_i = \frac{3\alpha_\phi K\dot{\varepsilon}_i^{\gamma\gamma} + (G/\sqrt{J_2})\mathbf{s}_i^{\alpha\beta}\dot{\varepsilon}_i^{\alpha\beta}}{9\alpha_\phi\alpha_\psi K + G} \tag{11}$$

Finally, the stress-strain relationship, in particle approximation form, is given by

$$\frac{D\boldsymbol{\sigma}_i^{\alpha\beta}}{Dt} = \boldsymbol{\sigma}_i^{\alpha\gamma}\dot{\boldsymbol{\omega}}^{\beta\gamma} + \boldsymbol{\sigma}_i^{\gamma\beta}\dot{\boldsymbol{\omega}}_i^{\alpha\gamma} + 2G\dot{\mathbf{e}}_i^{\alpha\beta} + K\dot{\varepsilon}_i^{\gamma\gamma}\delta_i^{\alpha\beta} - \dot{\lambda}_i\left[3\alpha_\psi K\delta^{\alpha\beta} + \frac{G}{\sqrt{J_2}}\mathbf{s}_i^{\alpha\beta}\right] \tag{12}$$

Where, the two first terms are the results from the Jaumann's stress rate tensor, the third and fourth terms refer to the elastic behavior, and the last term in the equation relates to the plastic deformation.

2.3. Soil-rock interaction

In this paper, we treat the rocks as rigid bodies and use the Newton's equation for rigid body dynamics to describe the rock motion. The force on each rock particle is computed by summing up the contribution from all the surrounding soil particles within the smooth kernel, as shown in Fig.1. Hence, rock particle r experiences a force per unit mass given by

$$f_r = \sum_{s \in SPs} f_{rs} \tag{13}$$

By the principle of equal and opposite action and reaction, the force exerted by a soil particle on each rock particle is obtained by $m_r f_r = -m_s f_s$. Thus we can estimate the force exerted on the whole moving body actually only by computing the force, f_s, exerted by a rock particle on a soil particle.

The rigid body dynamics including the translation and rotation equations are given by

$$M\frac{d\boldsymbol{V}}{dt} = \sum_{r \in RPs} m_r \boldsymbol{f}_r \text{ and } I\frac{d\boldsymbol{\Omega}}{dt} = \sum_{r \in RPs} m_r(\boldsymbol{r}_r - \boldsymbol{R}_0) \times \boldsymbol{f}_r \tag{14}$$

Each rock particle within the rigid body is moved in time by the velocity

$$\boldsymbol{u}_r = \boldsymbol{V} + \boldsymbol{\Omega} \times (\boldsymbol{r}_r - \boldsymbol{R}_0) \tag{15}$$

Besides, rock-rock contacts are computed by contact mechanics theory which is similar to the treatment in DEM[7].
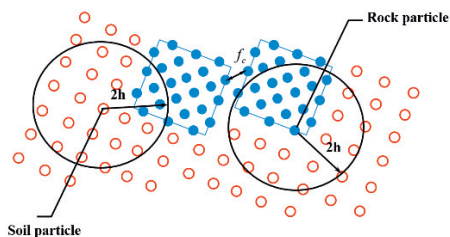

Fig.1. Sketch of soil-rock interaction.

Table 1. Soil parameters for test cases

No.	Soil parameters	T-Case 1	T-Case 2
1	Density	$2650 kg/m^3$	$2100 kg/m^3$
2	Elastic modulus	8.4MPa	15MPa
3	Poisson ratio	0.30	0.25
4	Cohesive strength	0kPa	11kPa

5	Friction angle	19.8°	20°
6	Dilatancy angle	0°	0°

3.Validation and Verification

Two test cases are implemented here to validate the method. Fig.2. shows the initial state of the two test cases, respectively. The soil parameters are listed clearly in table 1. The first test (T-Case 1) is about uniform non-cohesive soil slope failure. We simulated the gravitational flow following soil collapse. Comparing the final shape between experiment and SPH simulation,a good agreement is observed as shown in Fig.3. The other one (T-Case 2) is about uniform cohesive soil slope failure. Comparing the process of slope failure at three representative time instants between Bui's and our simulated result,the results of the comparison are satisfied as shown in Fig.4. Both of the two test cases can indicate that large deformation of soil during the post-failure process can be described very well through the SPH simulation.And the SPH methodhas a great application potential in studying the behavior of earth-rock aggregate.
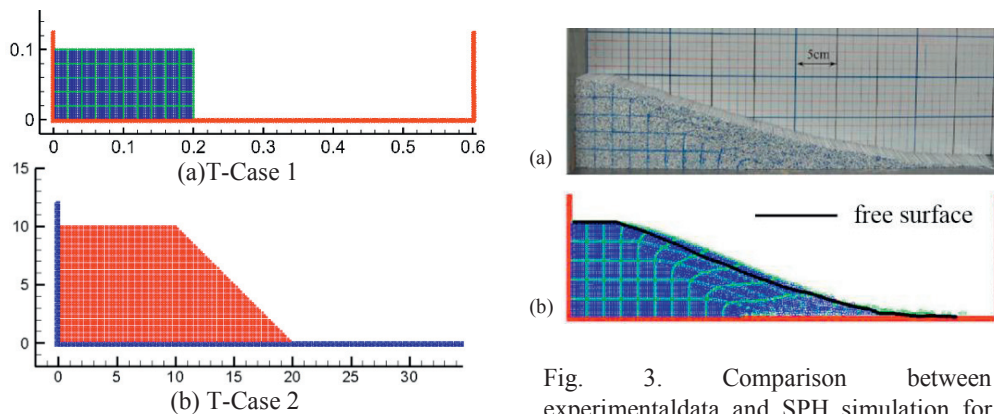

Fig.2. Initial state of test cases:
(a) T-Case 1, (b) T-Case 2

Fig. 3. Comparison between experimentaldata and SPH simulation for T-Case 1: (a) experimental result[1]; (b) our simulated result
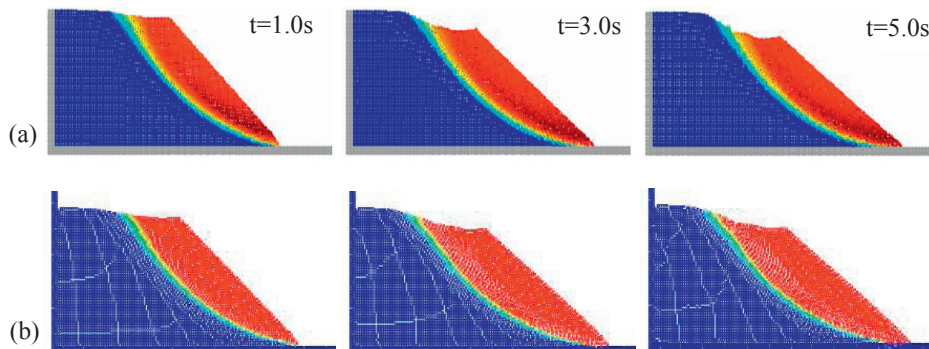

Fig.4 Contour plot of total displacement in the process of slope failure for T-Case 2:
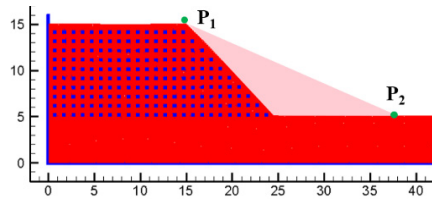a) SPH simulated result by Bui et al.[8]; (b) our simulated result

Fig.5. Model of earth-rock aggregate slope

Table 2. Specific parameter settings

No.	Parameters	Soil	Rock
1	Density	1800kg/m^3	1800kg/m^3
2	Elastic modulus	15MPa	50GPa
3	Poisson ratio	0.25	0.25
4	Cohesive force	11kPa	/
5	Friction angle	19.8°	/
6	Dilatancy angle	0°	/
7	Kinetic friction	/	0.65

Table 3. Summary of numerical cases

Schemes \ Slope (°)	25.0	27.5	30.0	32.5	35.0	37.5	40.0	42.5	45.0
Caseswithout rocks	N-Case 1	N-Case 2	N-Case 3	N-Case4	N-Case 5	N-Case 6	N-Case 7	N-Case 8	N-Case 9
Cases with small rocks (0.2m×0.2m)	S-Case 1	S-Case 2	S-Case 3	S-Case 4	S-Case 5	S-Case 6	S-Case 7	S-Case8	S-Case 9
Cases with huge rocks (0.4m×0.4m)	H-Case 1	H-Case 2	H-Case 3	H-Case4	H-Case 5	H-Case 6	H-Case 7	H-Case 8	H-Case 9

4. Results and discussions

We employ this method to study the behavior of earth-rock aggregate. Fig.5 shows the numerical model. The blue blocks stand for the rocks and the red zone represents the soil. For simplicity, well-distribution of rocks is set up here. P_1 located at the slope top and P_2 located at the slope toe are the probe points. They respectively imply the horizontal and vertical deformations of the slope. Specific parameters are set as table 3. Numerical experiments consist of 3 schemes, respectively corresponding to case without rocks, case with small rocks (0.2m×0.2m) and case with huge rocks (0.4m×0.4m). The value range of slope angle is from 25-45 degree. It's worth mentioning that all of the cases with rocks feature the same blending ratio 15.6%.Fig.6.shows the process of slope failure with slope angle of 45° at representative times, via contour plots of velocity magnitude for (a) the case without rocks and (b) the case with huge rocks. It shows that the proposed soil-rock interaction algorithm works well in the SPH framework.
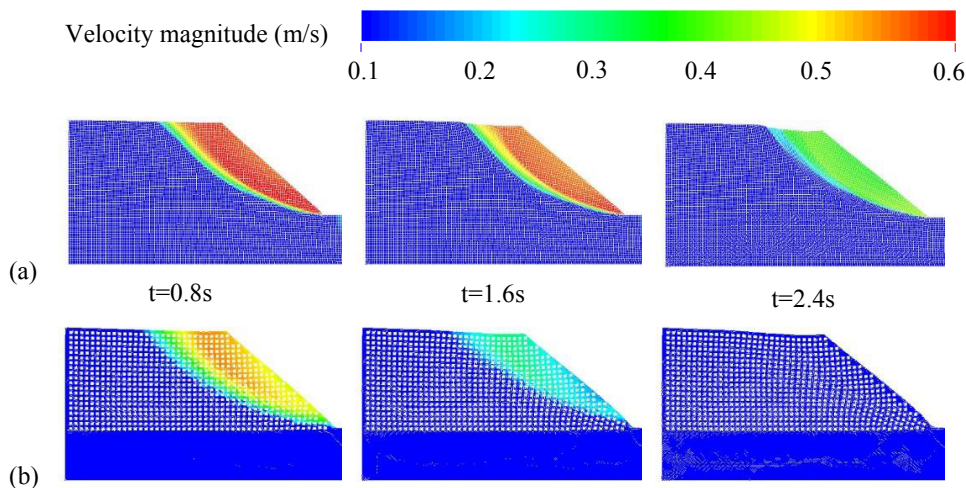

Fig.6 Contour plot of velocity magnitude in the process of slope failure with slope angle of 45°: (a) the case without rocks; (b) the case with small rocks
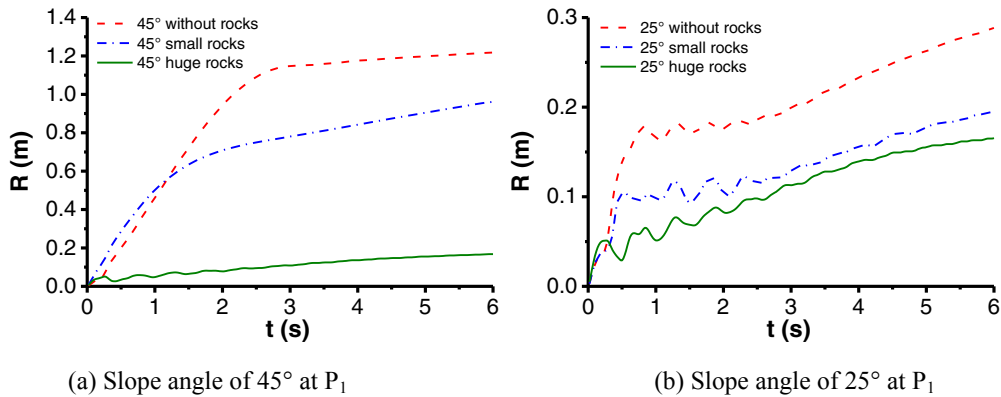
(a) Slope angle of 45° at P_1 (b) Slope angle of 25° at P_1

Fig.7. Comparison of the displacement-time curve at the slope top
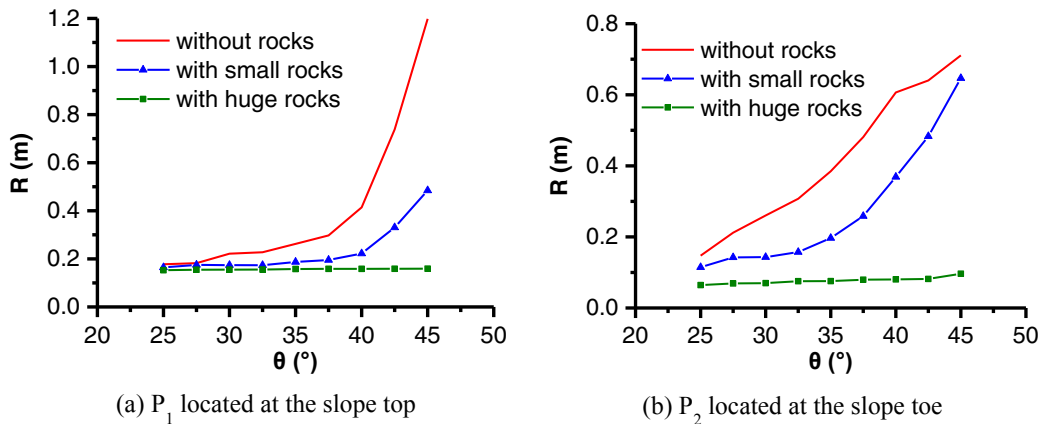P_1 with (a) 25° and (b) 45° slope angle respectively for three schemes

(a) P_1 located at the slope top   (b) P_2 located at the slope toe

Fig.8. The relationship between displacement R and slope angle θ at
(a) P_1 and (b) P_2 for three schemes at t=5.0s.

Fig.7 is the displacement-time graph at slope top P_1 for three schemes. According to Fig.7(a),when the slope angle is equal to 45°,the displacement value grows greatly over timeespeciallyin the absence of rocks corresponding to the scheme 1. However, for scheme 3 (with huge rocks), the displacement is almost invariable all the time. And for scheme 2 (with relative small rocks), the time evolution of displacement falls in between. They show that the rocks would block the soil plastic flow. And with the same blending ratio, the blockade effect would be enlarged with the increase of rock size.When the slope angle is equal to 25°, as shown in Fig.7(b), the same phenomena is observed althoughthe displacement varies weakly in either case.Itpartly suggests that the slope angle is another important factor that affects the whole deformation of landslide.

Let's focus on the typical time instant of 5.0s and study the relationship between the displacement and the slope angle. Fig.8shows the relationship between displacement R and slope angle θ at (a) P_1 and (b) P_2 for three schemes.As we known, with the increase of slope angle, the impact of soil resilience reduces gradually and so does the earth-rock aggregate. But even so, rocks could still block the development of landslide only if the rocksare big enough, as shown as the lower line for scheme 3 (with huge rocks) both in Fig.8(a) and Fig.8(b).For the other two schemes, the displacement grows greatly with the increase of the slope angle. Notably, the growing rate of displacement at $P_1$is

widening especially within the range of 40°~45°. But an opposite state is found at P_2 in the same range. We deduce that the soil plastic flow will occur at P_2but won't at P_1. When the slope angle is too large, the blockade of rocks at $P_2$is already not powerfulenough to hold the soil plastic flow.

Conclusions

Based on elastic-plastic soil model, we proposed a soil-rock interaction algorithm,which allowsto study more details in the post-failure of the earth-rock aggregate landslide.Numerical results obtained in this paper are qualitatively correct throughout. They showed that the rocks would block the development of landslide. With the same blending ratio, the blockade effect would be enlarged with the increase of stone size.The development of displacement at the slope toe is slightly with that at the slope top. The reason is just that plastic flow will occur at theslopetoebut not at theslopetop. And beyond that, the blockade effect of rocks is not apparent when the slope angle increasing to a certain degree.

Acknowledgements

References

[1] Ha H. Bui, Ryoichi Fukagawa, et al., Lagrangianmeshfree particles method (SPH) for large deformation and failure flows of geomaterial using elastic-plastic soil constitutive model. International Journal for Numerical and Analytical Methods in Geomechanics, 2008. 32(12): p. 1537-1570.

[2] Liu G.R., Liu M.B. Smoothed Particle Hydrodynamics: A Meshfree Particle Method [M]. World Scientific Publishing Co. Pte.Ltd, 2003.

[3] Opez, Y.R.L., D. Roose and C.R. Morfa, Dynamic refinement for SPH simulations of post-failure flow of non-cohesive soil, in the 7th International SPHERIC Workshop. 2012: Prato, Italy.

[4]Crespo AJC, Dominguez JM, Barreiro A, Gómez-Gesteira M and Rogers BD (2011)GPUs, a new tool of acceleration in CFD: Efficiency and reliability on Smoothed Particle Hydrodynamics methods. PLoS ONE 6 (6), e20685, doi:10.1371/journal.pone.0020685

[5]Gómez-Gesteira M, Rogers BD, Crespo AJC, Dalrymple RA, Narayanaswamy M and Dominguez JM (2012a) SPHysics - development of a free-surface fluid solver- Part 1: Theory and Formulations. Computers & Geosciences, doi:10.1016/j.cageo.2012.02.029.

[6]Gómez-Gesteira M, Crespo AJC, Rogers BD, Dalrymple RA, Dominguez JM and Barreiro A (2012b) SPHysics - development of a free-surface fluid solver- Part 2: Efficiency and test cases. Computers & Geosciences, doi:10.1016/j.cageo.2012.02.028.

[7] Ricardo Canelas, Rui M. L. Ferreira, et al., A generalized SPH-DEM discretization for themodelling of complex multiphasic free surface flows, in the 8th international SPHERIC workshop.2013: Trondheim, Norway.

[8] Ha H. Bui, K. Sako, et al., SPH-Based Numerical Simulations for Large Deformation of Geomaterial Considering Soil-Structure Interaction, in The 12th International Conference of International Association for Computer Methods and Advances in Geomechanics (IACMAG). 2008: Goa, India.